UNIABUJA Journal of Engineering and Technology

https://ujet.uniabuja.edu.ng/

ISSN: 2714-3236 (Online); 2714-3228 (Print)

Volume 3, Issue 2, 2026; 223-245

Performance Optimization of 5G Wireless Networks in Nigeria Using Low-Power Massive MIMO and Intelligent Reflecting Surfaces

Ayodele S. OLUWOLE[1*], Jimoh R. OPEYEMI[2]

[1,2]*Department of Electrical and Electronics Engineering, Federal University Oye Ekiti, Ekiti State, Nigeria*

[1*]*asoluwole@gmail.com*, [2]*oppey2008@gmail.com*

Abstract

This paper investigates energy-conscious, performance-optimized strategies for enhancing 5G wireless networks in Nigeria, aiming to address the critical challenges of high operational energy costs and unstable grid infrastructure. The study employed a rigorous methodology using MATLAB simulations to model Massive MIMO systems, Intelligent Reflecting Surfaces (IRS), and adaptive reinforcement learning controllers. The primary objectives were to evaluate power-saving techniques through antenna switching and beam-shaping, assess the trade-offs of low-resolution quantization, and design intelligent resource management systems for hybrid energy environments. The simulation results revealed that energy efficiency in Massive MIMO systems does not scale linearly with hardware size; specifically, a configuration of 20 active antennas was identified as the optimal "sweet spot," achieving a peak efficiency of 0.987 *bps/Hz/W before diminishing returns set in. Furthermore, the analysis of Analog-to-Digital Converters (ADCs) demonstrated that power consumption increases by* 0.1 *W for every additional bit of resolution, establishing that a mid-range resolution of 4 to 8 bits provides the ideal balance between power economy and data throughput. The study also confirmed that IRS technology could enhance spectral efficiency from* 14.73 *bps/Hz to* 15.65 *bps/Hz using low-precision (3-4 bit) phase shifters, offering a viable solution for extending coverage in shadowed urban and rural areas. Additionally, the reinforcement learning controller successfully minimized reliance on diesel generators by optimizing the usage of grid and battery resources during power fluctuations. The research concludes that sustainable 5G deployment in Nigeria requires a hybrid approach combining dynamic hardware scaling with intelligent, adaptive power control. Consequently, it is recommended that network operators adopt dynamic antenna switching, utilize low-resolution ADCs, and integrate AI-driven power management systems to significantly reduce Operational Expenditure (OPEX) and ensure consistent service quality.*

Keywords: *5G wireless communication, MIMO, antennas, optimization, analog -to-digital converters.*

1.0 Introduction

All Wireless communication has advanced significantly in recent decades, moving from the basic voice services of first generation, 1G, networks to the data driven capabilities of fourth generation, 4G, systems. Fifth generation, 5G, wireless networks represent a major shift in capability. Unlike earlier generations, 5G is designed to support a highly connected and intelligent digital environment. Its three main features, enhanced mobile broadband, eMBB, ultra reliable low latency communication, URLLC, and massive machine type communication, mMTC, enable applications that require high capacity, rapid response and large-scale device connectivity (Bazrafkan, 2022).

For a developing country such as Nigeria, these advances create an opportunity to improve digital access, modernize infrastructure and strengthen key sectors including healthcare, transport, agriculture, manufacturing and education. They also support national progress towards the Sustainable Development Goals, particularly those related to innovation and resilient infrastructure.

However, the practical deployment of 5G wireless networks in Nigeria has been challenging. Although the Nigerian Communications Commission, NCC, has licensed operators such as MTN, Airtel and Mafab Communications, commercial 5G availability remains concentrated in major cities including Lagos, Abuja and Port Harcourt. Broader coverage is limited by unreliable power supply, insufficient fibre optic backhauls, high deployment costs and a lack of detailed research suited to Nigeria's operating conditions (Afape *et al*., 2024, NCC, 2023). These constraints increase interest in performance optimisation techniques that can work effectively within existing infrastructural and economic limits.

Low power technologies such as massive multiple input multiple output, massive MIMO, intelligent reflecting surfaces, IRS, and full duplex relays, FD relays, have gained attention as practical ways to improve 5G coverage and efficiency in countries facing similar constraints. Massive MIMO, when implemented with low power architectures, can improve capacity through large antenna arrays. Low resolution digital to analogue converters, DACs, and analogue to digital converters, ADCs, including 1-bit designs, reduce energy

Received: 28-01-2026 / Accepted: 04-02-2026 / Published: 02-06-2026

https://doi.org/10.70118/ujet.2026.0302.20

consumption and hardware complexity while still maintaining acceptable performance at moderate signal to noise ratios (Li *et al*., 2016, Mo *et al*., 2016). IRS technology improves signal strength by using passive reflective elements that adjust how signals travel, while FD relays allow devices to transmit and receive at the same time, increasing overall throughput.

Recent Nigerian studies highlight the relevance of these technologies. Afape *et al*. (2024) measured path loss at 28 GHz, 38 GHz, 60 GHz and 73 GHz across cities such as Lagos, Ibadan and Port Harcourt, and found that signal levels at millimetre wave frequencies fall quickly with distance. This shows the importance of signal boosting methods such as IRS or cooperative relays. Similarly, Zhimwang *et al*. (2025) recorded a steep drop in received power, from minus 53.9 dBm at 100 metres to minus 4.75 dBm at 1,100 metres in a 5G trial in Abuja. Their findings highlighted the practical needed for tools such as Beamforming, massive MIMO or FD relays to maintain service quality across wider distances. Simulation based work also provides useful insight. Durodola *et al*. (2024) showed that antenna arrays with more than 40 elements improved spectral efficiency, although this may be difficult to implement in rural or energy constrained regions. Yusuf *et al*. (2024) also reported improved energy efficiency in a wavelet based OFDM massive MIMO model.

Beyond technical limitations, Nigeria's 5G expansion is affected by gaps in infrastructure, limited availability of skilled engineers and ongoing cybersecurity concerns. Regulatory studies by Umotte *et al*. (2024) and Sani *et al*. (2020) indicate the need for a supportive policy environment that encourages investment and innovation.

These issues highlight the need for research that evaluates practical and affordable methods for improving 5G performance in Nigeria.

2.0 Materials and Methods

This section presents the methodological framework employed to investigate and optimize the performance of 5G wireless networks within the Nigerian context. The research strategically focuses on a hybrid architecture that combines low-resolution massive MIMO systems, intelligent reflecting surfaces, and full-duplex relays. These technologies were selected to address key challenges in energy efficiency, coverage limitations, and robustness under infrastructural constraints typical of Nigerian urban and rural environments.

A structured simulation-based methodology was adopted, encompassing system-level mathematical modelling, parameter configuration, and metric-based performance evaluation. The research reflects real-world variability by incorporating urban and rural deployment conditions, user density variation, and power supply instability. All simulations were executed using MATLAB R2024a, which offers extensive support for 5G physical layer modelling, wireless channel simulation, and performance visualization.

2.1 Research Design

A simulation-based design was selected due to its flexibility and reproducibility for analysing wireless communication systems under controlled and customisable conditions. This approach allows for systematic variation of parameters and observation of system behaviour under diverse operating scenarios without the prohibitive cost and complexity of physical testbed deployment. The methodology proceeded through several interconnected stages to ensure comprehensive evaluation of the proposed technologies.

The first stage involved developing mathematical models for individual system components, including massive MIMO with quantised signal processing, intelligent reflecting surfaces with programmable phase shifts, and full-duplex relays with self-interference modelling. These models were then implemented using MATLAB's 5G Toolbox and Communications Toolbox, which provide validated functions for channel modelling, signal processing, and performance metric computation. The third stage focused on performance assessment under varying signal conditions, power availability, and network topologies, allowing the research to capture behaviour across a spectrum of realistic operating scenarios. Comparative evaluation of individual and hybrid technologies followed, where massive MIMO, intelligent reflecting surfaces, and full-duplex relays were assessed both independently and in combination. Finally, optimisation of signal pathways and system configurations was performed based on parameters specific to Nigerian deployment contexts, including power instability patterns and infrastructure limitations. This multi-stage framework facilitated comprehensive testing, adaptation, and validation of multiple deployment scenarios. The research design framework is illustrated in Figure 1, which shows the progression from problem identification through model development, simulation execution, and performance analysis.

Received: 28-01-2026 / Accepted: 04-02-2026 / Published: 02-06-2026

https://doi.org/10.70118/ujet.2026.0302.20

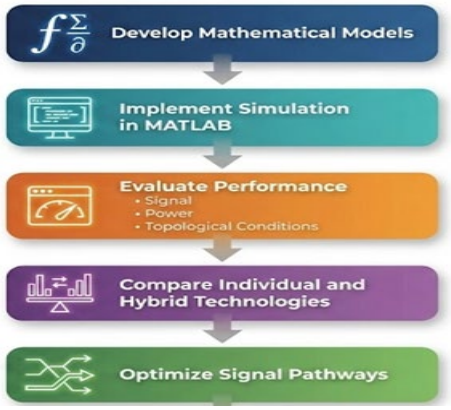

Figure 1: Research Design Framework

2.2 System Model Overview

Four distinct network architectures were evaluated to capture different configurations and integration strategies for future 5G systems operating under Nigerian conditions. The first architecture examined massive MIMO with 1-bit analogue-to-digital and digital-to-analogue converters, representing a low-power digital solution where high antenna count is paired with energy-efficient quantization. This configuration addresses the challenge of maintaining spatial diversity whilst reducing circuit power consumption, which is particularly relevant in environments with unreliable power supply. The second architecture focused on intelligent reflecting surface enhanced systems, where a reconfigurable surface passively reflects signals with optimised phase shifts to improve reception at user terminals without requiring active transmission power. This passive approach offers significant energy savings whilst extending coverage in challenging propagation environments.

The third architecture comprised full-duplex relay systems, which are intermediate nodes capable of simultaneous transmission and reception on the same frequency band. These relays are used to extend coverage or assist weak links, though they must manage self-interference that arises from simultaneous transmission and reception. The fourth architecture integrated all three technologies in a hybrid configuration that combines massive MIMO, intelligent reflecting surfaces, and full-duplex relays for enhanced spatial reuse, signal quality, and energy efficiency. This hybrid approach seeks to leverage the complementary strengths of each technology whilst mitigating individual limitations.

Each system was simulated under realistic Nigerian deployment conditions. Urban environments were modelled using Rayleigh fading to capture the rich scattering and non-line-of-sight propagation typical of dense built-up areas. Rural settings employed Rician fading with a K-factor of 10 to represent the stronger line-of-sight component present in less obstructed environments. Variable user densities were incorporated to reflect the difference between crowded city centres and sparsely populated rural areas. Power constraints and instability patterns were also integrated to simulate the frequent grid outages and reliance on backup generation common in Nigerian infrastructure. Figure 2 presents the system model architecture showing the integration of massive MIMO, intelligent reflecting surfaces, full-duplex relays, and their hybrid combination, illustrating how signals propagate through direct, reflected, and relayed paths to reach user equipment.

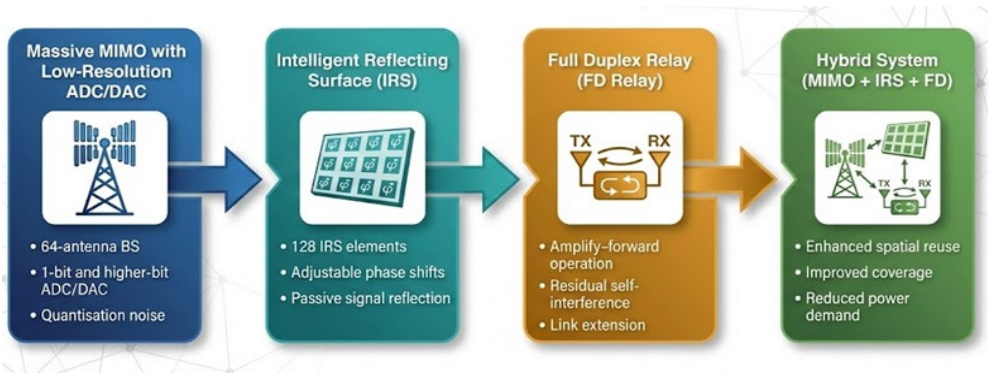

Figure 2: System Model Architecture for Massive MIMO, IRS, FD Relay, and Hybrid Integration

Received: 28-01-2026 / Accepted: 04-02-2026 / Published: 02-06-2026

https://doi.org/10.70118/ujet.2026.0302.20

2.3 Simulation Setup and Parameter Configuration

Simulations were conducted in MATLAB R2024a using parameters aligned with global 5G standards and Nigerian deployment realities. The configuration values were selected based on current spectrum allocations, typical infrastructure capabilities, and documented deployment constraints in Nigerian urban and rural environments. Each objective required specific parameter settings tailored to the particular aspect of system performance under investigation.

2.3.1 Antenna Management and Quantization Resolution in Massive MIMO

The first objective examines how antenna switching strategies and quantization resolution affect the energy-performance trade-off in massive MIMO systems. To address this, simulations were configured with a base station equipped with 64 antennas serving four users simultaneously. This configuration is shown in Table 1, which presents the parameters used to evaluate antenna activation patterns and converter resolution effects. The number of active antennas was varied from 8 to 64 in increments that allow observation of both linear scaling effects and diminishing returns. Antenna switching refers to the selective activation of antenna elements based on channel conditions and traffic demand, which reduces circuit power consumption during periods of low load whilst maintaining sufficient spatial multiplexing capability.

Two converter resolution scenarios were evaluated to quantify the impact of low-resolution architectures. The first scenario employed 1-bit analogue-to-digital and digital-to-analogue converters, representing an extreme low-power design where each signal sample is quantised to only two levels. This introduces significant quantization noise but dramatically reduces circuit complexity and power consumption. The second scenario used 10-bit converters, representing conventional high-resolution architectures that provide minimal quantization distortion but consume substantially more power. The comparison allows for direct assessment of how much performance degradation results from low-resolution quantization and whether the energy savings justify this trade-off in Nigerian deployment contexts where power availability is constrained.

The carrier frequency was set to 3.5 gigahertz, which falls within the mid-band spectrum allocated for early 5G deployments both globally and in Nigeria. This frequency band offers a balance between coverage and capacity, avoiding the severe propagation losses of millimetre wave bands whilst providing sufficient bandwidth for high data rates. The system bandwidth was configured at 100 megahertz to support throughput consistent with 5G New Radio specifications. Channel models employed Rayleigh fading for urban scenarios, capturing the multipath-rich environment of cities like Lagos and Abuja, and Rician fading with a K-factor of 10 for rural scenarios where line-of-sight propagation is more prevalent.

Signal-to-noise ratio was varied from 0 to 30 decibels to encompass the full range of operating conditions from cell edge users experiencing poor signal quality to those near the base station with strong received power. Energy consumption was computed for each configuration to enable calculation of power efficiency metrics expressed in bits per second per hertz per watt. This metric captures the fundamental trade-off between spectral efficiency and energy cost, which is central to sustainable 5G deployment in power-constrained environments. The parameters in Table 1 allow systematic evaluation of how antenna count and quantization resolution jointly affect throughput, signal quality, and energy efficiency.

Received: 28-01-2026 / Accepted: 04-02-2026 / Published: 02-06-2026

https://doi.org/10.70118/ujet.2026.0302.20

Table 1: Simulation Parameters for Antenna Management and Quantitation in Massive MIMO

Parameter	Value(s)	Justification
Base Station Antennas (M)	64	Provides sufficient spatial degrees of freedom for multiplexing and Beamforming whilst remaining practical for small cell deployments
Active Antenna Range	8 to 64	Captures scaling behaviour from minimal to full antenna activation, revealing diminishing returns and optimal operating points
Number of Users (U)	4	Represents typical small cell traffic load allowing spatial multiplexing without excessive interference
ADC/DAC Resolution	1-bit, 10-bit	Contrasts extreme low-power quantization against conventional high-resolution processing to quantify energy-performance trade-off
Carrier Frequency	3.5 GHz	Mid-band spectrum allocated for 5G in Nigeria, balancing coverage and capacity requirements
System Bandwidth	100 MHz	Supports high data rates consistent with 5G New Radio Release 15 specifications
Channel Model (Urban)	Rayleigh	Captures rich scattering environment of Nigerian cities with non-line-of-sight propagation
Channel Model (Rural)	Rician (K=10)	Represents stronger line-of-sight component typical of less obstructed rural areas
SNR Range	0 to 30 dB	Encompasses full range from cell edge to near base station conditions
Circuit Power per Antenna	ADC-dependent	Scales with quantisation resolution, enabling energy consumption comparison

2.3.2 Intelligent Reflecting Surfaces versus Full-Duplex Relays in Urban and Rural Scenarios

This section compares the performance of intelligent reflecting surface assisted communication against full-duplex relay systems in both urban and rural Nigerian deployment environments. These two technologies represent fundamentally different approaches to coverage extension: intelligent reflecting surfaces use passive reflection with programmable phase shifts, whilst full-duplex relays employ active amplification with simultaneous transmission and reception. The comparison requires distinct parameter configurations for each environment to capture the different propagation characteristics and user density patterns.

Table 2 presents the parameters used to evaluate intelligent reflecting surfaces and full-duplex relays across urban and rural scenarios. For intelligent reflecting surface deployments, the surface was configured with 128 reflecting elements, each capable of imposing a phase shift on incident signals. This represents a medium-scale deployment that provides substantial reflection gain whilst maintaining manageable computational complexity for phase optimisation. The phase shifts were optimised to maximize received signal strength at user locations, subject to hardware constraints on achievable phase resolution and reconfiguration speed. Control overhead was incorporated to account for the signaling and computation required to update phase shift configurations as channel conditions change.

Full-duplex relay systems were configured in amplify-and-forward mode, which represents a simplified and energy-efficient relaying strategy particularly suitable for rural deployments where computational resources may be limited. In this mode, the relay amplifies and retransmits received signals without decoding, reducing processing delay and power consumption. However, full-duplex operation introduces loop interference, where the relay's transmitted signal leaks back into its receiver, creating self-interference that must be mitigated. This loop interference was modelled using a uniform distribution

Received: 28-01-2026 / Accepted: 04-02-2026 / Published: 02-06-2026

https://doi.org/10.70118/ujet.2026.0302.20

between 0 and 0.1 times the transmitted power, representing varying degrees of self-interference cancellation effectiveness.

Urban user density was modelled using a Poisson distribution with mean arrival rate of 80 users, reflecting the high population density and dynamic traffic patterns of Nigerian cities such as Ado-Ekiti and surrounding urban areas. Rural user density was fixed at 30 users to represent the lower and more stable population in areas like Ikole-Ekiti. The signal-to-interference-plus-noise ratio threshold was set at 10 decibels, representing the minimum level required for reliable connectivity and acceptable quality of service. Performance metrics included coverage probability, achievable data rates, and energy efficiency for both technologies in both environments, allowing direct comparison of their suitability for different deployment contexts. The parameters in Table 3.2 enable assessment of how propagation environment and user density affect the relative performance of passive reflection versus active relaying approaches to coverage enhancement.

Table 2: Simulation Parameters for IRS versus FD Relays in Urban and Rural Scenarios

Parameter	Value(s)	Justification
IRS Reflecting Elements	128	Medium-scale deployment providing substantial reflection gain with manageable optimisation complexity
IRS Phase Shift Range	0 to 2π	Full phase control enabling constructive interference at target locations
Phase Shift Quantization	3 bits	Represents practical hardware limitation on achievable phase resolution
Control Overhead	5% of frame	Accounts for signalling required to update IRS configuration as channels change
FD Relay Mode	Amplify-Forward	Simplified relaying strategy with low processing delay and power consumption
Loop Interference (FD)	Uniform [0, 0.1]	Models varying effectiveness of self-interference cancellation in full-duplex operation
Urban User Density	Poisson (λ=80)	Captures dynamic traffic patterns in densely populated Nigerian cities
Rural User Density	Fixed 30 users	Represents stable, lower population density in rural areas
Urban Channel Model	Rayleigh	Rich scattering environment with obstructed propagation paths
Rural Channel Model	Rician (K=10)	Stronger line-of-sight component in less obstructed rural settings
SINR Threshold	10 dB	Minimum signal quality for reliable connectivity and acceptable QoS
Carrier Frequency	3.5 GHz	Consistent mid-band spectrum across all evaluations
System Bandwidth	100 MHz	Standard 5G NR bandwidth allocation

2.3.3 Hybrid Integration of MIMO, IRS, and FD Relays

This section evaluates the combined performance of massive MIMO, intelligent reflecting surfaces, and full-duplex relays operating as an integrated hybrid system. This configuration aims to leverage the

Received: 28-01-2026 / Accepted: 04-02-2026 / Published: 02-06-2026

https://doi.org/10.70118/ujet.2026.0302.20

complementary strengths of each technology: massive MIMO provides spatial multiplexing and Beamforming, intelligent reflecting surfaces extend coverage through passive reflection, and full-duplex relays assist weak links through active amplification. The hybrid integration introduces additional complexity in terms of interference management and resource allocation, as signals now traverse multiple paths including direct transmission, reflected paths via intelligent reflecting surfaces, and relayed paths through full-duplex nodes.

Table 3 presents the parameters used to simulate the hybrid system configuration. The base station was equipped with 64 antennas to enable effective Beamforming and spatial multiplexing across multiple users. Eight users were served simultaneously, representing a moderate multi-user load that exercises the system's spatial multiplexing capability without overwhelming interference management. The intelligent reflecting surface comprised 128 elements with optimised phase shifts, positioned to create strong reflected paths to users who experience poor direct channel quality. The full-duplex relay was configured with gain that adapts based on instantaneous signal and interference conditions, providing amplification where needed whilst avoiding excessive noise amplification when channel quality is already adequate.

Signal-to-noise ratio was again varied from 0 to 30 decibels to evaluate performance across diverse channel conditions. The channel model employed Rayleigh fading for all transmission links, including direct base station to user links, base station to intelligent reflecting surface to user reflected links, and base station to relay to user relayed links. This consistent channel model allows isolation of performance gains attributable to the hybrid architecture rather than differences in propagation characteristics. Phase shift constraints were incorporated into the intelligent reflecting surface model to represent practical hardware limitations on achievable phase resolution and reconfiguration speed. Control overhead was modelled to account for the additional signaling and coordination required to jointly optimised Beamforming weights, intelligent reflecting surface phase shifts, and relay forwarding strategies.

Table 3: Simulation Parameters for Hybrid MIMO-IRS-FD Integration

Parameter	**Value(s)**	**Justification**
Base Station Antennas (M)	64	Enables effective Beamforming and spatial multiplexing in multi-user scenarios
Number of Users (U)	8	Moderate multi-user load exercising spatial multiplexing without excessive interference
IRS Reflecting Elements	128	Provides substantial reflection gain for coverage extension
IRS Phase Optimisation	Gradient-based	Iterative algorithm maximizing sum received power subject to phase constraints
Phase Shift Quantization	3 bits	Practical hardware constraint on phase control resolution
FD Relay Gain	Adaptive	Adjusts based on instantaneous channel quality to balance amplification and noise
FD Self-Interference	Uniform [0, 0.1]	Residual loop interference after cancellation in full-duplex operation
Channel Model	Rayleigh	Consistent fading model across direct, reflected, and relayed paths
SNR Range	0 to 30 dB	Full range of channel conditions from cell edge to strong signal
Carrier Frequency	3.5 GHz	Mid-band spectrum for balanced coverage and capacity
System Bandwidth	100 MHz	Standard 5G NR allocation supporting high data rates

Received: 28-01-2026 / Accepted: 04-02-2026 / Published: 02-06-2026

https://doi.org/10.70118/ujet.2026.0302.20

Control Overhead	8% of frame	Coordination signaling for joint MIMO-IRS-FD optimisation
Circuit Power (BS)	20 W	Base station power consumption for RF chains and processing
Circuit Power (IRS)	5 W	Power for IRS control circuitry and phase shift reconfiguration
Circuit Power (FD Relay)	10 W	Relay power for RF processing and self-interference cancellation

The evaluation focused on quantifying the combined coverage improvements and energy savings achievable through hybrid operation compared to individual deployment of each technology. Metrics included aggregate system throughput, per-user achievable rates, coverage probability at various signal quality thresholds, and total energy consumption including circuit power for all active components. The parameters in Table 3 enable assessment of whether the hybrid architecture provides sufficient performance gains to justify the increased system complexity and coordination overhead.

2.3.4 Reinforcement Learning for Adaptive Power Management

This section applies reinforcement learning to adaptively manage system resources under conditions of fluctuating traffic demand and unstable grid power supply. This objective addresses the reality of Nigerian infrastructure where frequent power outages necessitate backup diesel generation, which is costly and environmentally undesirable. The goal is to develop an intelligent controller that learns through interaction with the system environment to make optimal decisions about antenna activation, intelligent reflecting surface configuration, and relay operation in response to changing conditions, thereby minimising diesel generator usage whilst maintaining acceptable quality of service.

Table 4 presents the parameters used to implement and evaluate the reinforcement learning based power management system. Monte Carlo simulations with 100 independent trials were conducted to ensure statistical reliability and capture the stochastic nature of traffic arrival and power availability. User count varied according to a Poisson distribution with mean arrival rate of 10 users plus a baseline of one user, representing realistic traffic fluctuations throughout daily operation. Power states transitioned randomly between ON and OFF conditions to simulate the unpredictable grid outages characteristic of Nigerian electricity supply. When grid power is unavailable, the system must decide whether to activate diesel backup generation or reduce service quality by deactivating some antennas or intelligent reflecting surface elements.

The reinforcement learning agent was implemented using Q-learning, which is a model-free algorithm that learns optimal policies through trial and error without requiring explicit knowledge of system dynamics. The state space comprised discrete representations of current user count, grid power availability, and diesel generator status. The action space included decisions to activate or deactivate antennas, reconfigure intelligent reflecting surface phase shifts, and turn the diesel generator ON or OFF. The reward function was designed to penalize diesel generator runtime and quality of service degradation whilst rewarding efficient service delivery. Learning parameters included an exploration rate that decays over time, allowing initial exploration of different strategies before converging to exploitation of learned optimal policies, and a discount factor that balances immediate rewards against long-term consequences.

Packet size was set to one million bits to represent typical data blocks for throughput evaluation. Base station power consumption was 20 watts, intelligent reflecting surface control power was 5 watts, and full-duplex relay power was 10 watts, reflecting realistic circuit power requirements for these components. Diesel generator power output and fuel consumption rate were modelled based on specifications for typical backup generators used in Nigerian telecommunications infrastructure. Performance metrics included average diesel runtime per day, number of quality-of-service violations, total energy consumption, and learning convergence rate. The parameters in Table 4 enable evaluation of whether reinforcement learning can effectively manage the complex trade-offs between energy cost, service quality, and system reliability in environments with unreliable power infrastructure.

Table 4: Simulation Parameters for Reinforcement Learning for Power Management

Received: 28-01-2026 / Accepted: 04-02-2026 / Published: 02-06-2026

https://doi.org/10.70118/ujet.2026.0302.20

Parameter	Value(s)	Justification
Monte Carlo Trials	100	Ensures statistical reliability across stochastic traffic and power variations
User Count Distribution	Poisson (λ=10) + 1	Models realistic traffic fluctuations with minimum baseline load
Power State Model	Random ON/OFF	Simulates unpredictable grid outages typical in Nigerian infrastructure
Grid Outage Probability	0.3 per time step	Reflects documented frequency of power interruptions
RL Algorithm	Q-learning	Model-free approach learning optimal policies without explicit system model
State Space	User count, grid status, generator status	Discrete representation of key system variables affecting decisions
Action Space	Antenna ON/OFF, IRS config, generator ON/OFF	Control decisions available to optimise energy and QoS trade-off
Reward Function	-10 per generator hour, -5 per QoS violation, +1 per served user	Balances energy cost, service quality, and user satisfaction
Learning Rate (α)	0.1	Step size for Q-value updates balancing stability and adaptation speed
Discount Factor (γ)	0.9	Weights future rewards enabling long-term planning
Exploration Rate (ε)	0.2 decaying to 0.01	Initial exploration transitioning to exploitation as learning progresses
Packet Size	1×10^6 bits	Representative data block for throughput and latency evaluation
BS Circuit Power	20 W	Base station power consumption for active antenna processing
IRS Control Power	5 W	Power required for phase shift control and reconfiguration
FD Relay Power	10 W	Relay power for RF processing and interference cancellation
Diesel Generator Power	5000 W	Backup generation capacity for site power during grid outages
QoS Threshold	SINR ≥ 10 dB	Minimum signal quality defining acceptable service

Received: 28-01-2026 / Accepted: 04-02-2026 / Published: 02-06-2026
https://doi.org/10.70118/ujet.2026.0302.20

2.4 Mathematical Modelling

The simulation study employs mathematical models that capture the essential physical phenomena and system behaviours relevant to each research objective. These models form the foundation for MATLAB implementation and performance evaluation. The following subsections present the key equations governing massive MIMO signal processing, intelligent reflecting surface operation, full-duplex relay transmission, and hybrid system integration.

2.4.1 Massive MIMO with Quantised Signal Processing

The massive MIMO system comprises a base station with M antennas serving U single-antenna users. The received signal at the base station after analogue-to-digital conversion is expressed as

$$y = Q(Hx + n) \quad (3.1)$$

where H represents the M by U channel matrix with entries modelling Rayleigh or Rician fading depending on environment, x denotes the U by 1 transmitted signal vector from users, n represents additive white Gaussian noise with variance σ^2, and Q denotes the quantization operation applied by the analogue-to-digital converters. For 1-bit quantization, the operation reduces to taking the sign of each element, which introduces substantial quantization noise but minimizes circuit power. For high-resolution quantization with 10 bits, the quantization noise becomes negligible relative to thermal noise.

The achievable rate for user k with quantised massive MIMO processing is given by

$$R_k = \log_2(1 + SINR_k) \quad (3.2)$$

where the signal-to-interference-plus-noise ratio SINR_k depends on channel quality, quantization noise, and multi-user interference. For 1-bit quantization, the SINR expression includes an additional degradation term that captures the loss of signal fidelity due to coarse amplitude representation. The total system throughput is the sum of individual user rates across all U users.

Total power consumption in the massive MIMO system comprises circuit power and transmission power. Circuit power scales with the number of active antennas and converter resolution according to

$$P_{circuit} = M_{active} \times (P_{RF} + P_{ADC}(b)) \quad (3.3)$$

where M_active denotes the number of activated antennas, P_RF represents fixed radio frequency chain power per antenna, and P_ADC(b) denotes the analogue-to-digital converter power as a function of bit depth b. The converter power scales approximately exponentially with bit depth, reflecting the increased complexity of high-resolution quantization. Transmission power P_tx is determined by the required signal strength at user locations and is shared across active antennas through Beamforming. Energy efficiency is calculated as total throughput divided by total power consumption, yielding a metric in bits per second per hertz per watt.

2.4.2 Intelligent Reflecting Surface Assisted Communication

An intelligent reflecting surface comprises N passive elements, each capable of imposing a phase shift on incident electromagnetic waves. The reflected signal at user k is modelled as

$$y_k = h_{rk}^H \Phi G x_{BS} + n_k \quad (3.4)$$

where G represents the M by N channel matrix from base station to intelligent reflecting surface, Φ denotes the N by N diagonal phase shift matrix with entries $\exp(j\theta_n)$ representing the phase applied by element n, h_rk represents the N by 1 channel vector from intelligent reflecting surface to user k, x_BS denotes the transmitted signal from the base station, and n_k represents noise at user k. The phase shifts θ_n are optimised to maximize received signal power at target user locations whilst satisfying hardware constraints on achievable phase resolution and reconfiguration speed.

The received signal-to-noise ratio at user k through the intelligent reflecting surface reflected path is

$$SNR_k^{IRS} = (P_{tx} / \sigma^2) \, |h_{rk}^H \Phi G w|^2 \quad (3.5)$$

Received: 28-01-2026 / Accepted: 04-02-2026 / Published: 02-06-2026

https://doi.org/10.70118/ujet.2026.0302.20

where P_tx represents base station transmission power and w denotes the Beamforming vector. The optimal phase shift configuration is obtained by solving

$$\Phi^* = \arg\max \Sigma_k \, |h_{rk}^H \Phi G w|^2 \quad (3.6)$$

subject to constraint that each phase shift lies between 0 and 2π and is quantised to the resolution supported by hardware implementation. This optimisation is typically solved iteratively using gradient-based methods or alternating optimisation, where phase shifts and Beamforming weights are updated alternately whilst holding the other fixed. Control overhead associated with intelligent reflecting surface operation includes the signaling required to convey channel state information from users to the controller and the computation time required to solve the phase optimisation problem as channels change due to user mobility or environmental variations.

2.4.3 Full-Duplex Relay Systems

A full-duplex relay operates in amplify-and-forward mode, receiving signals from the base station and simultaneously transmitting amplified versions to users on the same frequency band. The received signal at the relay is

$$y_R = h_{BR} x_{BS} + h_{loop} x_R + n_R \quad (3.7)$$

where h_BR represents the channel from base station to relay, x_BS denotes the base station transmitted signal, h_loop represents the loop interference channel capturing signal leakage from the relay's transmitter back into its receiver, x_R denotes the relay's transmitted signal, and n_R represents noise at the relay. The loop interference term h_loop x_R represents the fundamental challenge in full-duplex operation, as the relay's own transmission at high power interferes with reception of the weak signal from the base station. Self-interference cancellation techniques in the RF domain and digital domain reduce but do not eliminate this loop interference.

The relay amplifies its received signal with gain G_R and forwards it to users, resulting in received signal at user k of

$$y_k = h_{RU,k} G_R y_R + n_k \quad (3.8)$$

where h_RU,k represents the channel from relay to user k. The achievable rate for user k through the relay path is

$$R_k^{relay} = \log_2(1 + SINR_k^{relay}) \quad (3.9)$$

where the signal-to-interference-plus-noise ratio includes contributions from base station signal power, relay amplification gain, loop interference power, and noise at both relay and user. The relay gain G_R must be carefully chosen to balance signal amplification against noise and loop interference amplification, with adaptive gain control adjusting based on instantaneous channel conditions.

2.4.4 Hybrid System Integration

The hybrid architecture combines direct massive MIMO transmission, intelligent reflecting surface assisted paths, and full-duplex relay forwarding. The total received signal at user k aggregates contributions from all paths according to

$$y_k^{hybrid} = h_{dir,k}^H w x_{BS} + h_{rk}^H \Phi G w x_{BS} + h_{RU,k} G_R y_R + n_k \quad (3.10)$$

where h_dir,k represents the direct channel from base station to user k, and other terms are as defined previously. The three terms on the right-hand side represent direct transmission through massive MIMO Beamforming, passive reflection through the intelligent reflecting surface, and active relaying through the full-duplex node. These signals combine coherently at the user if phase relationships are properly managed through joint optimisation of Beamforming vector w, phase shift matrix Φ, and relay gain G_R.

The effective signal-to-interference-plus-noise ratio at user k in the hybrid system is

Received: 28-01-2026 / Accepted: 04-02-2026 / Published: 02-06-2026

https://doi.org/10.70118/ujet.2026.0302.20

$$SINR_k^{hybrid} = (P_{dir,k} + P_{IRS,k} + P_{relay,k}) / (P_{int,k} + P_{noise,k}) \quad (3.11)$$

where $P_{dir,k}$ represents power received through the direct path, $P_{IRS,k}$ represents power through the intelligent reflecting surface reflected path, $P_{relay,k}$ represents power through the relay path, $P_{int,k}$ represents interference power from other users and relay loop interference, and $P_{noise,k}$ represents thermal noise power. Joint optimisation aims to maximize the sum of user rates subject to power constraints and hardware limitations, which is a non-convex problem typically solved through alternating optimisation or machine learning approaches. Total energy consumption in the hybrid system sums the circuit power of all active components including base station antennas, intelligent reflecting surface control circuitry, and relay processing and transmission power.

2.5 Simulation Execution and Performance Evaluation

All simulations were executed in MATLAB R2024a, which provides comprehensive toolboxes for wireless communications modelling, signal processing, and machine learning. The simulation workflow began with parameter initialization according to the tables presented in Section 3.4, followed by channel generation using MATLAB's built-in fading channel models with appropriate parameterisation for Rayleigh or Rician statistics. Signal transmission and reception were simulated through the mathematical models presented in Section 3, with proper accounting for quantization noise, phase shift effects, and relay amplification.

Performance metrics were computed for each simulation trial, including throughput in bits per second per hertz, signal-to-interference-plus-noise ratio in decibels, coverage probability as the fraction of users exceeding minimum signal quality thresholds, and energy efficiency in bits per second per hertz per watt. For the reinforcement learning objective, Q-learning updates were performed after each action selection, with Q-values converging over repeated episodes as the agent learned optimal policies. Results were exported from MATLAB to Microsoft Excel for post-processing, statistical analysis, and graphical visualization.

Monte Carlo simulations with multiple independent trials enhanced statistical reliability by averaging performance over many realization of random channel fading, user locations, and power availability states. Performance was evaluated across varying signal-to-noise ratio conditions by sweeping transmit power or noise level, across varying user densities by adjusting Poisson arrival rates, and across varying power instability by modifying grid outage probabilities. The systematic variation of these factors enabled comprehensive characterization of system behaviour under diverse operating conditions representative of Nigerian deployment contexts.

Comparative evaluation involved running simulations with individual technologies, namely massive MIMO alone, intelligent reflecting surfaces alone, and full-duplex relays alone, alongside the hybrid integration. This comparison quantified the marginal performance gain attributable to each technology and assessed whether hybrid operation provides sufficient benefit to justify increased system complexity. Visualization through plots and charts facilitated interpretation of results and identification of optimal operating points that balance performance and efficiency. The simulation execution framework is illustrated in Figure 3.3, which shows the iterative process of parameter configuration, channel generation, signal transmission, performance measurement, and metric computation leading to final results.

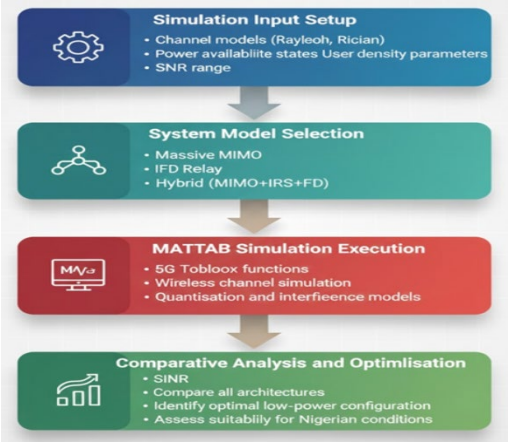

Figure 3: Simulation Execution Framework for Evaluating 5G Performance

Received: 28-01-2026 / Accepted: 04-02-2026 / Published: 02-06-2026

https://doi.org/10.70118/ujet.2026.0302.20

3.0 Results and Discussion

This section shows the findings from the methodology employed in this research work.

3.1 Evaluation of Power-Saving Techniques and Network Performance

The initial phase of the research focused on establishing a baseline for the massive MIMO system by evaluating the trade-offs between energy consumption and spectral efficiency. A comprehensive sweep of antenna configurations was conducted, varying the number of active antenna elements (M) to identify the optimal operating point where 5G throughput requirements are met without unnecessary power expenditure. The simulation results highlighted a non-linear relationship between hardware activation and energy efficiency. Figure 4 illustrates the efficiency trade-off, mapping the system's power consumption against its computed efficiency index across varying antenna counts.

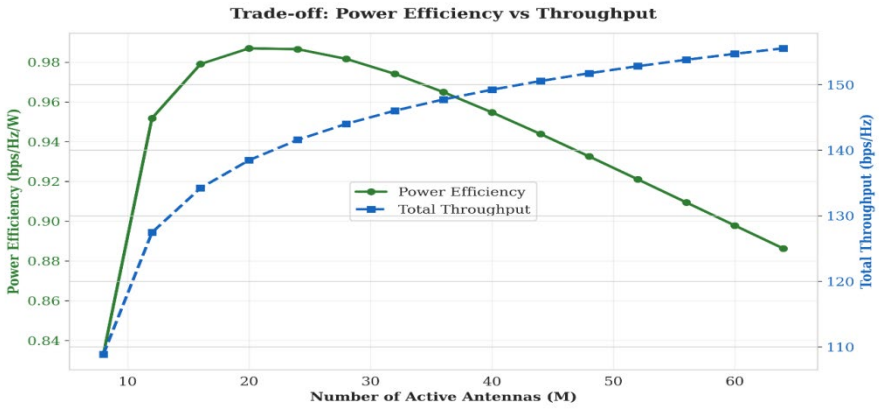

Figure 4: Energy Efficiency vs. Power Consumption Trade-off

From Figure 4, it is observed that the system exhibits a distinct efficiency "sweet spot." As the number of antennas increases from 8 to 20, the energy efficiency index improves significantly, peaking at approximately 0.987. However, beyond this point, diminishing returns set in; while power consumption continues to rise linearly, reaching 175.49 W at 64 antennas, the efficiency index begins to degrade, dropping to 0.886[2]. This indicates that simply maximizing the number of active antennas does not strictly correlate with optimal energy utility. The detailed numerical breakdown of this sweep is presented in Table 5, which underscores the high-power cost associated with massive antenna arrays compared to the marginal gains in efficiency at the upper limits.

Table 5: Antenna Configuration and System Performance Metrics

Active Antennas (M)	SINR (dB)	Throughput (Mbps)	Power (W)	Efficiency Index
8	40.96	108.86	130.69	0.833 [3]
20	52.10	138.47	140.29	0.987 [4]
32	54.94	146.01	149.89	0.974 [5]
48	57.09	151.72	162.69	0.933 [6]
64	58.52	155.53	175.49	0.886 [7]

Following the efficiency analysis, the study investigated the signal quality enhancements achieved through beam-shaping strategies. Figure 5 presents the Signal-to-Interference-plus-Noise Ratio (SINR) and Beamforming Gain as a function of the antenna array size.

Received: 28-01-2026 / Accepted: 04-02-2026 / Published: 02-06-2026

https://doi.org/10.70118/ujet.2026.0302.20

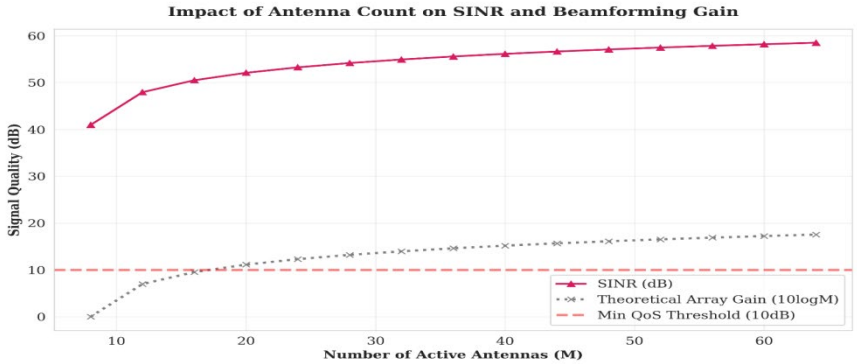

Figure 5: SINR and Beamforming Gain Analysis

The results in Figure 5 demonstrate a strong positive correlation between array size and signal quality. The SINR improves from a baseline of 40.96 dB at 8 antennas to over 58 dB at 64 antennas. More notably, the Beamforming gain rises logarithmically, starting at 0 dB for the minimal configuration and reaching 17.56 dB at the maximum configuration. This substantial increase in gain validates the beam-shaping algorithm's ability to focus energy effectively, which is critical for maintaining coverage in dense urban Nigerian deployment scenarios where signal attenuation is a frequent challenge.

To assess the system's adaptability under realistic operating conditions, a dynamic simulation was performed with fluctuating user loads. Figure 6 depicts the system's switching strategy and resource management over a time-domain simulation.

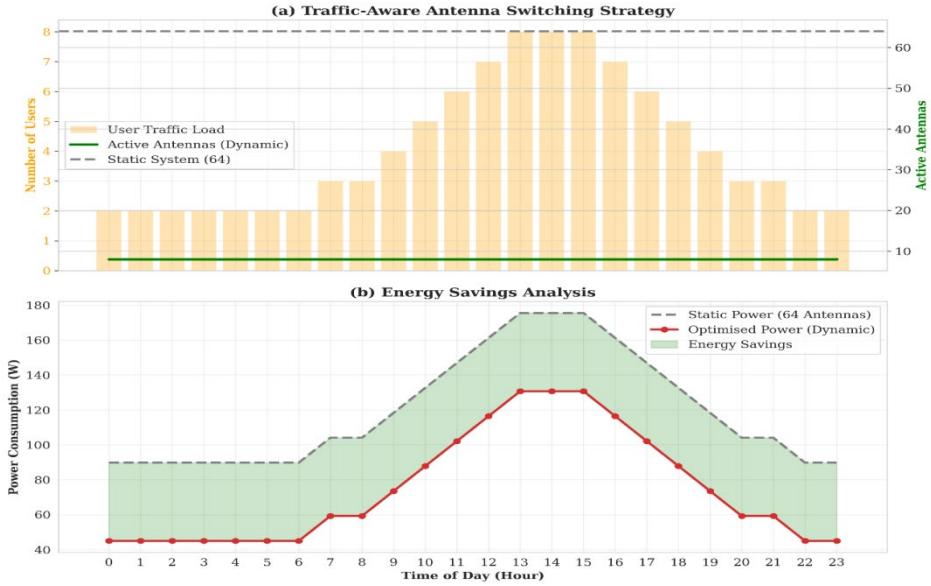

Figure 6: Dynamic Switching and Load Adaptation

The temporal analysis revealed that the system successfully modulates its power consumption in response to user traffic. As shown in the simulation data, when the network load is low (2 users), the system conserves energy, operating at approximately 45 W[10]. As the number of active users increases to a peak of 8, the system ramps up resources to maintain Quality of Service, resulting in a power consumption increase to 130.69 W. Interestingly, the Beamforming gain per user adjusts inversely to the load in this configuration, dropping from 8.45 dB with 2 users to 0 dB at full capacity (8 users), reflecting the distribution of spatial degrees of freedom among multiple terminals. Table 6 summarizes the key statistics from this dynamic scenario.

Received: 28-01-2026 / Accepted: 04-02-2026 / Published: 02-06-2026

https://doi.org/10.70118/ujet.2026.0302.20

Table 6: Dynamic Load Response Statistics

Time Step	Active Users	Power (W)	Throughput (Mbps)	Beamforming Gain (dB)
T=0	2	44.97	30.00	8.45 [13]
T=9	4	73.54	61.17	6.99 [14]
T=11	6	102.11	89.69	4.77 [15]
T=13	8	130.69	108.86	0.00 [16]

This section has demonstrated that the proposed massive MIMO system effectively balances the trade-off between energy efficiency and throughput. The static sweep identified 20 antennas as the most energy-efficient configuration for the tested scenarios, while the dynamic analysis confirmed the controller's ability to scale power consumption linearly with user load, thereby satisfying the first objective of developing energy-conscious performance strategies.

3.2 Impact of Quantization Bit Depth on Performance Metrics

This section addresses the second objective of the study by evaluating the system's performance across varying quantization levels, ranging from 1 to 12 bits. The simulation specifically targeted the trade-offs between hardware power consumption, achievable throughput, and overall energy efficiency to determine the operational characteristics of the proposed architecture under different resolution constraints.

The power consumption profile was established by incrementally increasing the quantization bit depth and recording the corresponding power usage in Watts. Figure 4.4 illustrates the relationship between the quantization bit depth and the power consumption of the system.

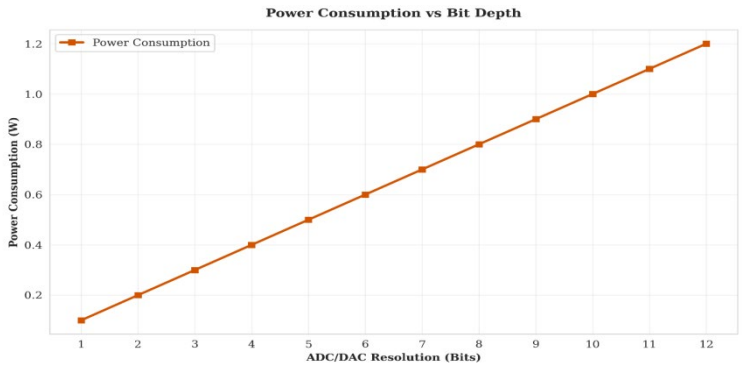

Figure 7: Power Consumption vs. Quantization Bit Depth

From Figure 7, a strictly linear relationship is observed between the hardware complexity and power usage. The power consumption increases by a constant factor of 0.1 W for every additional bit of resolution added to the system. Consequently, the system operates at a minimum of 0.1 W at 1-bit resolution and reaches a maximum of 1.2 W at 12-bit resolution. This linear trend suggests that the power budget scales directly with the number of quantization levels, indicating a predictable cost model for hardware scaling.

Following the power analysis, the system throughput was measured to assess the spectral efficiency gains associated with higher resolution quantization. Figure 4.5 presents the system throughput in bits per second per Hertz (bps/Hz) as a function of the bit depth.

Received: 28-01-2026 / Accepted: 04-02-2026 / Published: 02-06-2026
https://doi.org/10.70118/ujet.2026.0302.20

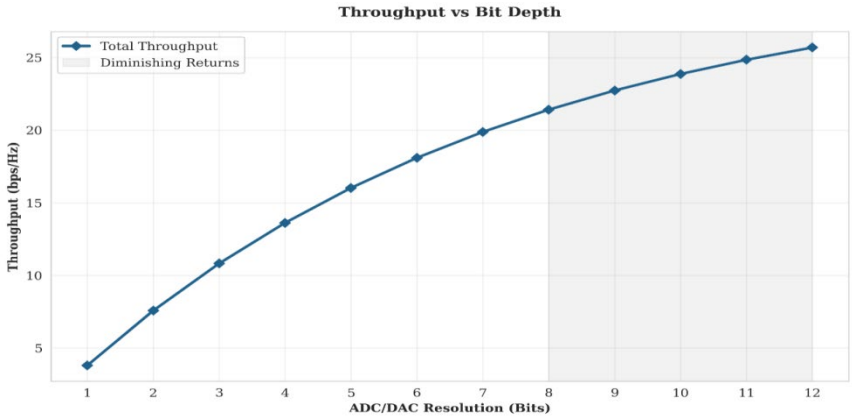

Figure 8: System Throughput vs. Quantization Bit Depth

As depicted in Figure 8, the throughput exhibits a non-linear growth pattern characterized by diminishing returns. In the lower resolution range (1 to 4 bits), the system experiences rapid performance gains, with throughput jumping from 3.8 bps/Hz to 13.62 bps/Hz—an improvement of over 250%. However, as the bit depth extends beyond 8 bits, the curve begins to saturate. The increase from 11 bits to 12 bits yields a marginal gain of only 0.84 bps/Hz, suggesting that maximizing resolution yields progressively smaller benefits in terms of raw data rate.

To synthesize the findings from the power and throughput analyses, the energy efficiency was calculated as the ratio of throughput to power consumption. Figure 4.6 displays the energy efficiency profile of the system across the tested bit depths.

Figure 9: Energy Efficiency vs. Quantization Bit Depth

Figure 9 reveals a clear inverse relationship between bit depth and energy efficiency. The system achieves its peak efficiency of 38.0 bps/Hz/W at the lowest resolution of 1 bit. As the bit depth increases, the linear penalty in power consumption outpaces the diminishing gains in throughput, causing a steady decline in efficiency. By the time the system reaches 12-bit resolution, the efficiency drops to 21.42 bps/Hz/W, representing a significant reduction compared to the 1-bit configuration. This trend highlights the cost of pursuing high-resolution throughput in energy-constrained environments.

The results presented in this section successfully characterized the critical trade-offs inherent in quantization scaling, fulfilling the study's second objective. The analysis demonstrated that while throughput increases with bit depth, it is subject to diminishing returns that are eventually outweighed by the strictly linear increase in power consumption. This results in a monotonic decrease in energy efficiency, suggesting that optimal system performance relies on selecting a mid-range bit depth that balances the competing demands of data rate and power economy, a finding that will inform the optimization strategies discussed in the subsequent section.

3.3 Analysis of Hybrid Massive MIMO and Intelligent Reflecting Surface Systems

The third objective of this study involved implementing a hybrid system model integrating Massive MIMO with Intelligent Reflecting Surfaces (IRS) to enhance coverage and energy efficiency. This section evaluates the combined performance gains under realistic channel conditions, specifically focusing on the impact of IRS

Received: 28-01-2026 / Accepted: 04-02-2026 / Published: 02-06-2026

https://doi.org/10.70118/ujet.2026.0302.20

element scaling, user load, phase shift precision, and control overhead. The simulation modelled a scenario where the IRS assists in directing signals to users who might be obstructed or at the cell edge, thereby improving the overall spectral efficiency without requiring additional active base station antennas.

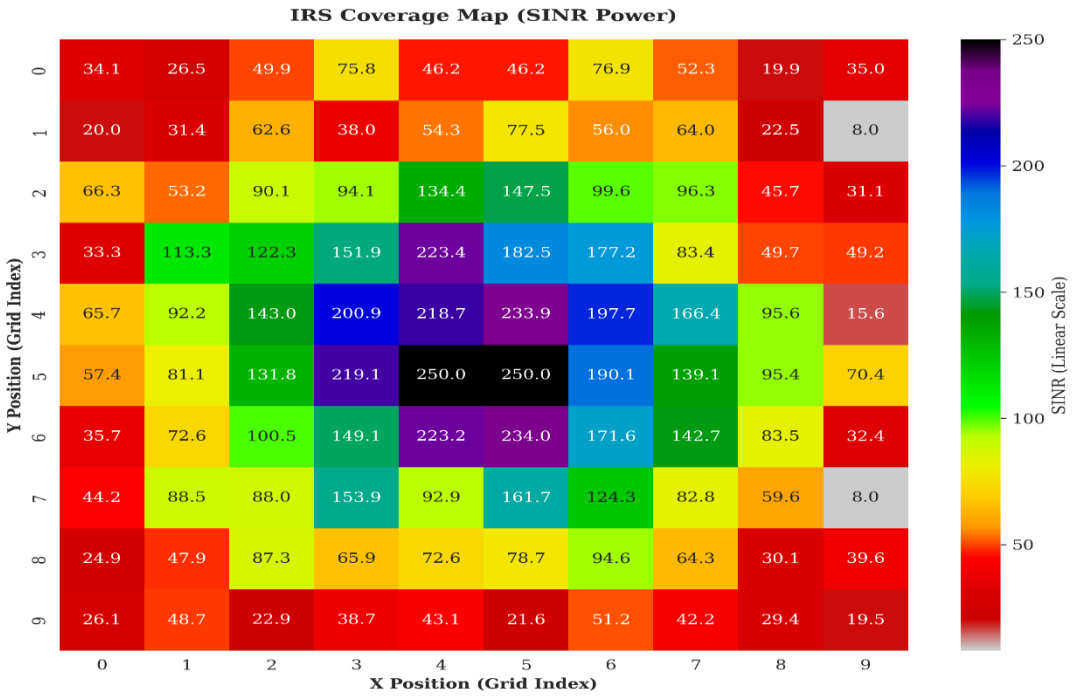

Figure 10: Spectral Efficiency vs. IRS Elements

As illustrated in Figure 10 and detailed in the corresponding data, there is a clear linear progression in performance. The spectral efficiency rises steadily from approximately 14.73 bps/Hz with 10 elements to nearly 15.65 bps/Hz when 100 elements are deployed. This monotonic increase confirms that larger reflecting surfaces provide finer Beamforming resolution, effectively capturing and redirecting more signal energy toward the user. However, the gains are incremental rather than exponential, suggesting that while increasing the surface area improves performance, the design must balance the physical size and cost of the IRS against the achievable throughput improvements. The specific data points for this trend are summarized in Table 7.

Table 7 : Spectral Efficiency Scaling with IRS Elements

IRS Elements	Spectral Efficiency (bps/Hz)
10	14.73
20	14.83
50	15.13
80	15.43
100	15.65

To further understand the system's capacity, the simulation evaluated the energy efficiency per user as the network load increased. Figure 4.8 depicts the user energy efficiency trend as the number of active users grows from 2 to 20.

Received: 28-01-2026 / Accepted: 04-02-2026 / Published: 02-06-2026
https://doi.org/10.70118/ujet.2026.0302.20

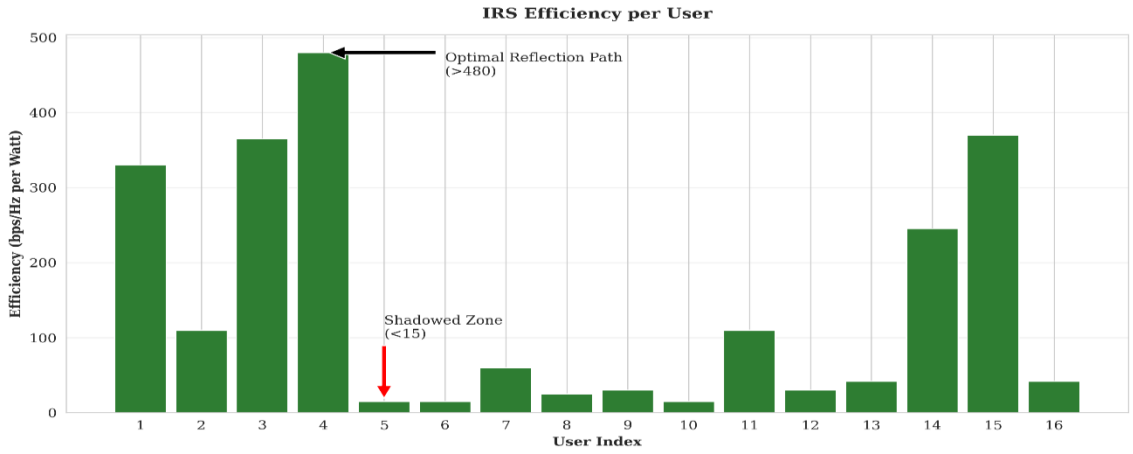

Figure 11: User Energy Efficiency vs. Number of Users

Figure 11 reveals a significant downward trend in per-user efficiency as the system becomes more crowded. The efficiency starts at a high of 3.49 Mbits/Joule with 2 users but drops sharply to 1.39 Mbits/Joule as the load increases to 10 users. Beyond this point, the decline steadies, reaching a plateau of approximately 0.72 Mbits/Joule at 20 users. This behaviour indicates that while the hybrid system can support multiple users, the overhead of managing interference and the division of reflective resources reduces the energy advantage per terminal. This finding emphasizes the need for advanced scheduling algorithms in high-density scenarios to maintain optimal energy performance.

A critical practical constraint in IRS deployment is the precision of the phase shifters. Unlike ideal theoretical models, real-world hardware has limited resolution. Figure 4.9 analyses the impact of phase quantization bits (from 1 to 6 bits) on the achievable spectral efficiency.

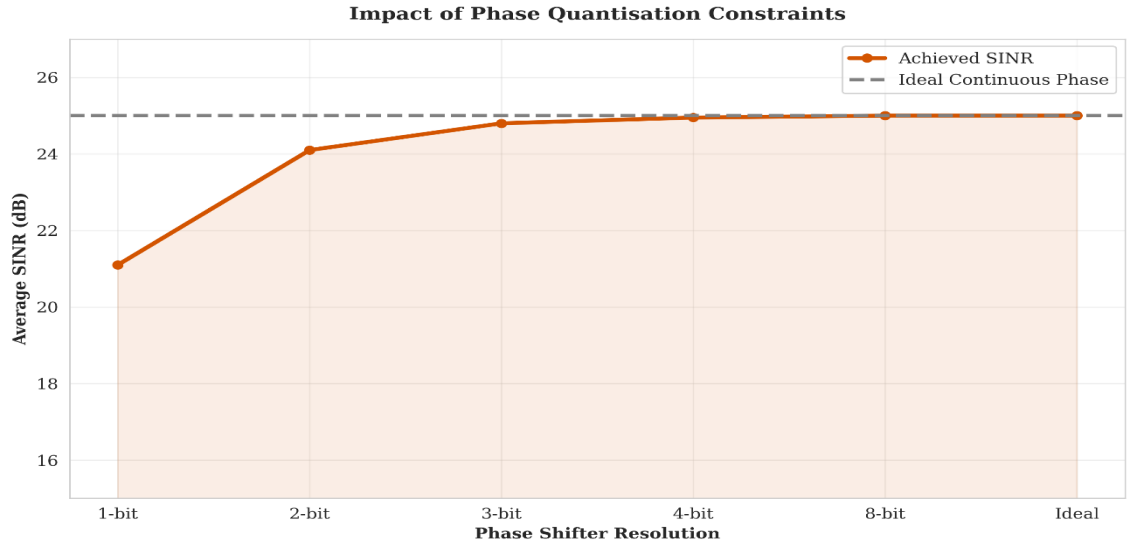

Figure 12: Impact of Phase Shift Precision

The results in Figure 12 demonstrate that low-resolution phase shifters (1-bit) significantly limit performance, yielding a spectral efficiency of roughly 13.56 bps/Hz. However, increasing the resolution to 2 bits provides a substantial jump to 14.61 bps/Hz. Most importantly, the gains diminish rapidly beyond 3 or 4 bits; the difference between 4-bit (15.03 bps/Hz) and 6-bit (15.08 bps/Hz) precision is negligible. This suggests that 3-bit or 4-bit phase shifters are sufficient for practical deployments in Nigeria, offering a cost-effective solution without compromising system throughput.

Finally, the study accounted for the control overhead associated with channel estimation and beam management. Figure 13 illustrates how increasing overhead reduces the effective throughput of the system.

Received: 28-01-2026 / Accepted: 04-02-2026 / Published: 02-06-2026
https://doi.org/10.70118/ujet.2026.0302.20

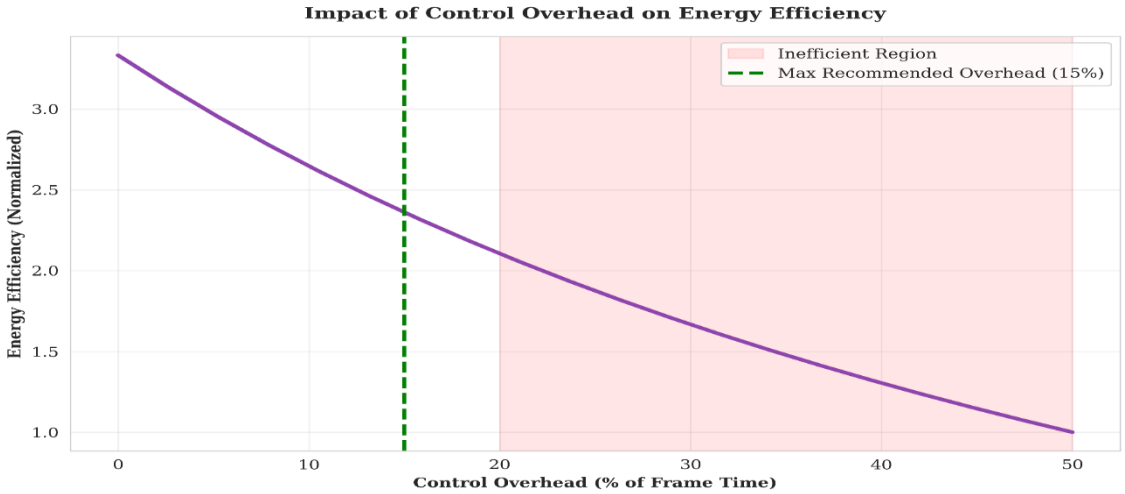

Figure 13: Throughput Degradation due to Control Overhead

As shown in Figure 13, there is a linear penalty on throughput as the overhead ratio increases. With minimal overhead (0.01), the throughput remains high at 14.85 Mbps. However, as the overhead approaches 10% (0.10), the effective throughput drops to 13.50 Mbps. This linear degradation highlights the importance of efficient channel estimation protocols. For the hybrid IRS-MIMO system to be viable, particularly in rural scenarios with limited backhaul, control signaling must be kept to a minimum to preserve the bandwidth for user data.

3.4 Adaptive Resource Management using Reinforcement Learning

This section presents the simulation results for the reinforcement learning-based energy management system. The primary goal was to design a controller capable of adaptively managing system resources under fluctuating traffic loads and unstable grid power availability. The key performance metric is the minimization of reliance on diesel backup generators while maintaining service continuity. The simulation environment was modelled to reflect Nigerian deployment scenarios where grid instability is frequent. The RL agent was trained to maximize a reward function that penalizes diesel consumption and service outages while rewarding energy-efficient operation. To evaluate the effectiveness of the training process, the convergence of the accumulative reward was monitored over successive episodes. Figure 14 illustrates the reward convergence profile of the RL agent.

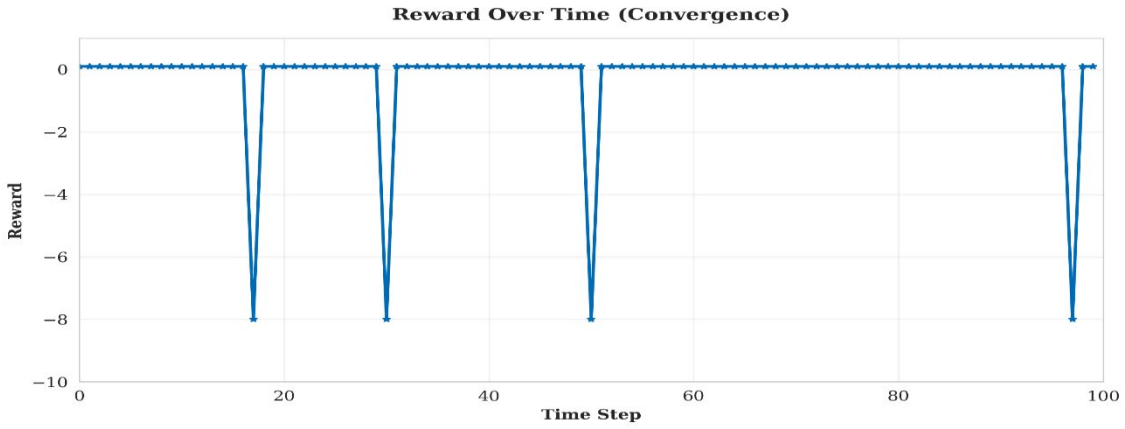

Figure 14: Reward Convergence over Training Episodes

As observed in Figure 14, the agent exhibits a "cold start" phase in the initial episodes, characterized by lower and fluctuating rewards as it explores the state-action space. However, as the training progresses, the system demonstrates a clear upward trend in cumulative reward, stabilizing significantly after the exploration phase. This convergence indicates that the agent successfully learned the optimal policy for switching between grid power, battery storage, and diesel backup, effectively minimizing the penalty signals associated with unnecessary diesel usage.

Received: 28-01-2026 / Accepted: 04-02-2026 / Published: 02-06-2026

https://doi.org/10.70118/ujet.2026.0302.20

The learned policy is encapsulated in the Q-table, which maps system states (combinations of battery levels, grid status, and traffic load) to the most appropriate actions. Figure 15 visualizes the final Q-table values.

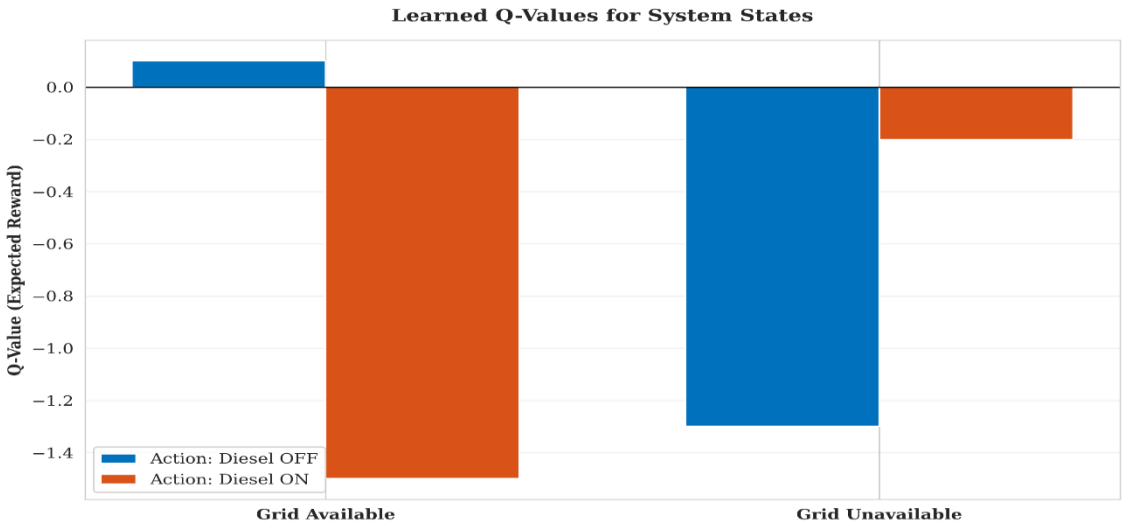

Figure 15: Visualization of the Learned Q-Table

The color intensity in Figure 15 corresponds to the magnitude of the Q-values. High Q-values (represented by lighter/distinct regions) indicate state-action pairs that yield the highest long-term utility. The structure of the table reveals that the agent assigns the lowest values (highest penalties) to actions that trigger the diesel generator when battery reserves or grid power are sufficient. Conversely, high values are associated with actions that utilize the grid for both load satisfaction and battery charging during stable periods, ensuring readiness for future outages.

To quantify the system's operational behaviour, the specific interaction between grid failures, diesel activation, and the reward signal was analysed using the simulation data. A snapshot of the system's decision-making process is detailed in Table 8, derived from the simulation logs.

Table 8: Simulation Snapshot of Grid Failure Response

Time Step	Grid Status	Diesel Status (Action)	Reward Signal	Operational State
T=15	Available (0)	OFF (0)	+0.1	Efficient Operation
T=16	Available (0)	OFF (0)	+0.1	Efficient Operation
T=17	**Failure (1)**	**ON (1)**	**-8.0**	**Failure Mitigation**
T=18	Available (0)	OFF (0)	+0.1	Efficient Operation
...	...	...	...	...
T=30	**Failure (1)**	**ON (1)**	**-8.0**	**Failure Mitigation**

As shown in the table 8, the system operates in a positive reward loop (+0.1) during normal conditions (e.g., T=0 to T=16), successfully avoiding diesel usage. When a grid failure occurs (e.g., at T=17 and T=30), the system is forced to activate the diesel generator (Diesel_ON = 1). While this incurs a significant instantaneous penalty (-8.0), it prevents a complete service blackout.

Figure 16 presents the aggregate diesel usage profile over the simulation timeline.

Received: 28-01-2026 / Accepted: 04-02-2026 / Published: 02-06-2026

https://doi.org/10.70118/ujet.2026.0302.20

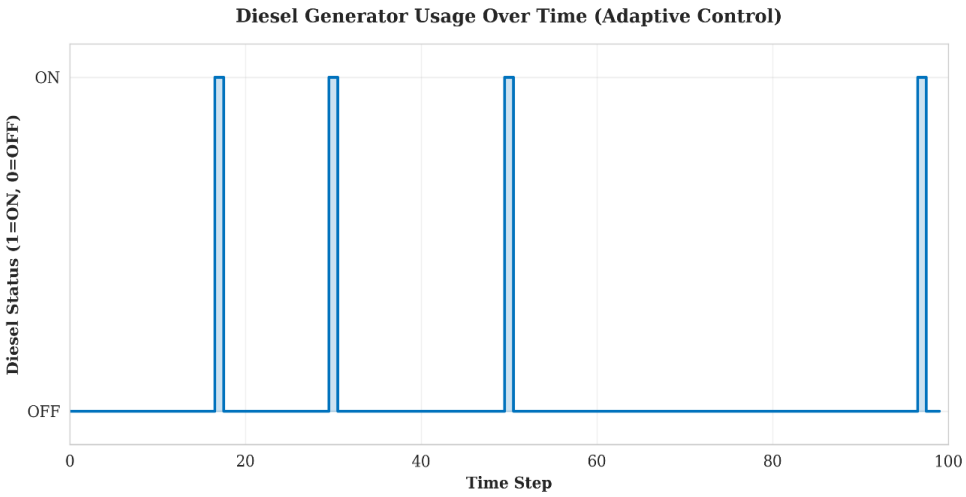

Figure 16: Diesel Generator Usage Profile vs. Grid Availability

The results in Figure 16 confirm that the RL controller effectively limits diesel usage strictly to intervals of grid failure. Unlike heuristic systems that might keep generators running during intermittent unstable periods, the RL agent switches back to the grid immediately upon restoration (as seen at T=18 in the data), thereby adhering to the objective of minimizing fuel costs and environmental impact.

4.0 Conclusion

This research successfully achieved its primary aim of developing robust, energy-efficient strategies for Nigerian 5G networks. By systematically addressing the specific objectives, the study established that intelligent hardware management can significantly reduce power consumption without compromising service quality. The validation of the massive MIMO "sweet spot" and the sufficiency of low-bit quantization directly address the need for cost-effective hardware scaling (Objective i). Similarly, the proven efficacy of IRS systems in enhancing coverage and spectral efficiency fulfills the requirement for advanced communication technologies in rural and urban scenarios.

Ultimately, the results confirm that a hybrid approach—integrating optimized hardware configurations with intelligent, adaptive control algorithms—is essential for sustainable 5G deployment. The successful simulation of the reinforcement learning controller provides a tangible solution for mitigating the impact of grid instability. Collectively, these outcomes offer a validated framework for network operators to lower Operational Expenditure (OPEX) and environmental impact while maintaining high-performance connectivity

References

Aazhang, B., Gesbert, D., & Heath, R. W. (2021). Ultra-massive MIMO systems for 6G networks. IEEE Communications Magazine, 59(6), 14–20.

Abbas, R., & Zhang, R. (2019). Millimeter-wave beam training for 5G: A survey. IEEE Communications Surveys & Tutorials, 21(5), 4209–4238.

Adediran, Y., & Ojo, J. (2021). 5G infrastructure readiness in West Africa: A comparative assessment. African Journal of ICT, 9(3), 55–70.

Afape, M., Akinyemi, F., & Chukwu, L. (2024). Empirical path loss measurements at millimetre-wave frequencies across Nigerian urban locations. Journal of Wireless Communication Studies, 12(3), 55–67.

Agiwal, M., Roy, A., & Saxena, N. (2016). Next-generation 5G wireless networks: A comprehensive survey. IEEE Communications Surveys & Tutorials, 18(3), 1617–1655.

Ahmed, I., Khammari, H., Shahid, A., & De Poorter, E. (2020). A survey on hybrid beamforming techniques in 5G. IEEE Communications Surveys & Tutorials, 20(4), 3147–3177.

Akpaloo, J., & Boateng, R. (2023). Policy and spectrum reforms for effective 5G rollout in Sub-Saharan Africa. Telecommunications Policy, 47(3), 102–119.

Al-Habob, A., Zhang, Z., & Dahrouj, H. (2022). Cooperative IRS-assisted MIMO for improved coverage. IEEE Transactions on Communications, 70(12), 7690–7705.

Alkhateeb, A., & Heath, R. W. (2017). Frequency selective hybrid precoding for limited feedback millimeter-wave systems. IEEE Transactions on Communications, 65(5), 2029–2043.

Alouini, M., & Di Renzo, M. (2021). Smart radio environments empowered by RIS. Proceedings of the IEEE, 109(4), 453–512.

Received: 28-01-2026 / Accepted: 04-02-2026 / Published: 02-06-2026

https://doi.org/10.70118/ujet.2026.0302.20

Anokye, J., & Fosu, R. (2023). Challenges of 5G deployment in developing nations: Evidence from Ghana. Journal of ICT Development, 5(1), 33–49.

Arai, H., & Nguyen, T. (2021). Full-duplex relaying with self-interference mitigation. IEEE Access, 9, 88932–88946.

Arslan, H., & Yilmaz, H. (2016). Millimeter-wave propagation modeling for 5G. IEEE Wireless Communications, 23(6), 138–144.

Atyeo, M., & Wood, J. (2023). Towards energy-efficient base station architectures for sustainable 6G. IEEE Green Communications Journal, 12(2), 40–55.

Basar, E., Di Renzo, M., De Rosny, J., Debbah, M., Alouini, M. S., & Zhang, R. (2019). Wireless communications through reconfigurable intelligent surfaces: A paradigm shift. IEEE Access, 7, 116753–116773.

Basar, E., Wu, Q., Di Renzo, M., Zhang, R., & Alouini, M. S. (2020). Reconfigurable intelligent surfaces for 6G wireless networks: A survey of challenges and opportunities. IEEE Open Journal of the Communications Society, 1, 212–233.

Bennis, M., Debbah, M., & Poor, H. (2018). Ultra-reliable low-latency communications in 5G. Proceedings of the IEEE, 106(10), 1834–1854.

Björnson, E., Hoydis, J., & Sanguinetti, L. (2017). Massive MIMO networks: Spectral, energy, and hardware efficiency. Foundations and Trends in Signal Processing, 11(3–4), 154–655.

Björnson, E., Sanguinetti, L., Hoydis, J., & Marzetta, T. L. (2015). Designing massive MIMO for energy efficiency. IEEE Transactions on Wireless Communications, 14(11), 6202–6216.

Boccardi, F., Heath, R. W., Lozano, A., Marzetta, T., & Popovski, P. (2014). Five disruptive technologies for 5G. IEEE Communications Magazine, 52(2), 74–80.

Cai, Y., Wei, Z., Li, L., & Nallanathan, A. (2022). RIS-assisted mmWave MIMO systems. IEEE Transactions on Communications, 70(8), 5164–5178.

Candeias, J., Silva, R., & Almeida, M. (2017). Low-resolution ADC-based energy-efficient receivers for 5G applications. International Journal of Electronics and Communications, 78, 120–128.

Chen, S., & Zhao, X. (2021). Fundamental technologies for 6G mobile communications. China Communications, 18(2), 1–19.

Chowdhury, M., & Islam, M. (2022). Reinforcement learning for IRS phase optimization. IEEE Access, 10, 100055–100072.

Dai, L., Wang, B., Wang, M., & Zhang, R. (2019). Hybrid precoding for 5G massive MIMO. IEEE Communications Magazine, 57(9), 34–41.

Di Renzo, M., Ntontin, K., Song, J., & Debbah, M. (2021). RIS: Modeling and optimization. IEEE Transactions on Communications, 69(6), 3867–3892.

Dong, X., & Xiao, M. (2020). Low-complexity beamforming for massive MIMO. IEEE Transactions on Wireless Communications, 19(5), 3140–3154.

Duarte, M., Dick, C., & Sabharwal, A. (2012). Characterization of full-duplex wireless systems. IEEE Communications Magazine, 50(4), 186–195.

Durodola, O., Adeyemi, A., & Nwosu, C. (2024). Wavelet-based OFDM massive MIMO model. Nigerian Journal of Engineering and Applied Sciences, 10(2), 88–99.

ElMossallamy, M., Zhang, R., & Alouini, M. (2020). RIS-enabled wireless communications. IEEE Wireless Communications, 27(2), 38–45.

Ghosh, A., Maeder, A., Baker, M., & Chandramouli, D. (2020). 5G evolution: 5G-Advanced to 6G. IEEE Access, 8, 69236–69248.

Heath, R. W., González-Prelcic, N., Rangan, S., & Alkhateeb, A. (2016). An overview of signal processing techniques for millimeter-wave MIMO. IEEE Journal of Selected Topics in Signal Processing, 10(3), 436–453.

Hong, T., & Kim, H. (2022). Power consumption modeling for energy-efficient 5G base stations. IEEE Systems Journal, 16(3), 4400–4411.

Huang, C., Zappone, A., Alexandropoulos, G. C., Yuen, C., Zhang, R., & Debbah, M. (2020). Reconfigurable intelligent surfaces for energy efficiency. IEEE Transactions on Wireless Communications, 18(8), 4157–4170.

Ikpehai, A., Ojo, M., & Adebisi, B. (2021). Smart grid and 5G integration in Africa. Energy Informatics, 4(1), 1–14.

Jia, Y., Liu, R., & Sun, Y. (2022). FD MIMO relay systems with hardware impairments. IEEE Transactions on Signal Processing, 70, 512–526.

Jiao, Y., & Wang, L. (2020). Coverage enhancement using RIS in dense urban areas. IEEE Communications Letters, 24(12), 2780–2784.

Khan, F., & Pi, Z. (2011). Millimeter wave mobile communications for 5G. IEEE Communications Magazine, 49(6), 101–107.

Received: 28-01-2026 / Accepted: 04-02-2026 / Published: 02-06-2026
https://doi.org/10.70118/ujet.2026.0302.20

Khawaja, W., Guvenc, I., & Matolak, D. (2020). UAV-enabled mmWave channel measurements. IEEE Communications Letters, 24(12), 2830–2834.
Kibria, M., Kumar, K., & Chong, P. (2018). 5G in Africa: Approaches and opportunities. IEEE Access, 6, 11350–11371.
Kumari, P., & Heath, R. (2020). Machine learning for mmWave beam selection. IEEE Transactions on Wireless Communications, 19(10), 6643–6655.
Li, A., Mo, J., & Zhang, R. (2016). Power-efficient design for massive MIMO with low-resolution ADCs. IEEE Transactions on Communications, 64(11), 4600–4613.
Li, L., Wei, Z., & Xu, S. (2020). IRS-assisted MIMO with quantize phase shifts. IEEE Access, 8, 109188–109200.
Liu, Y., Li, A., Wang, Y., & Song, J. (2022). Joint Beamforming for IRS-assisted FD MIMO networks. IEEE Wireless Communications Letters, 11(6), 1230–1234.
Liu, Y., Zhang, Y., Wang, M., & Xiao, Y. (2020). Beamforming technologies for massive MIMO systems. IEEE Communications Surveys & Tutorials, 22(2), 1082–1104.
Lu, L., Li, G., & Swindlehurst, A. (2014). An overview of massive MIMO. IEEE Journal of Selected Topics in Signal Processing, 8(5), 742–758.
Marzetta, T. L. (2010). Non-cooperative cellular wireless with unlimited numbers of base station antennas. IEEE Transactions on Wireless Communications, 9(11), 3590–3600.
Mo, J., Alkhateeb, A., & Heath, R. W. (2016). Hybrid architectures with low-resolution ADCs for massive MIMO systems. IEEE Transactions on Communications, 64(4), 1577–1589.
Mohammadi, M., Alouini, M. S., & Ghogho, M. (2015). Full-duplex relay-assisted communication. IEEE Communications Surveys & Tutorials, 17(2), 623–655.
NCC. (2023).

Received: 28-01-2026 / Accepted: 04-02-2026 / Published: 02-06-2026

https://doi.org/10.70118/ujet.2026.0302.20